Molecular recognition between guanine and cytidine in a head group of nucleolipid monolayer forming the top leaflet of a hybrid bilayer supported at a gold (111) electrode

Julia Alvarez-Malmagro[a,b], ZhangFei Su[b], J.Jay Leitch[b], Francisco Prieto[a *], Manuela Rueda[a *], Jacek Lipkowski[b *]

[a] Department of Physical Chemistry, University of Seville, C/Profesor García González nº 2, 41012 Seville, Spain.

[b] Department of Chemistry, University of Guelph, Guelph, Ontario, Canada N1G 2W1.

Corresponding authors:

Francisco Prieto: dapena@us.es

Manuela Rueda: marueda@us.es

Jacek Lipkowski: jlipkows@uoguelph.ca

Abstract

A hybrid bilayer lipid membrane (hBLM), composed of a self-assembled, 1-hexadecanethiol monolayer interior leaflet and a 1,2-dipalmitoyl-sn-glycero-3-cytidine nucleolipid monolayer exterior leaflet, was deposited at the surface of a gold (111) electrode. This system was used to investigate the molecular recognition reaction between the cytosine moieties of the lipid head group with guanine molecules present within the bulk electrolyte solution. Electrochemical measurements and photon polarization modulation infrared reflection absorption spectroscopy (PM IRRAS) were employed to characterize the system and determine the extent of the molecular recognition reaction. The capacitance of the hBLM-covered gold

electrode was very low (~1 μF cm^{-2}), therefore the charge density at the gold surface and changes in the static electric field acting on the membrane were small. Changing the electrode potential had a minimal effect on formation of the complex between the cytosine moiety guanine molecule due to the small changes in the static electric field across the membrane. This behavior favored formation of the complex between guanine and cytosine.

Keywords: hybrid bilayer lipid membrane (hBLM), 1,2-dipalmitoyl-sn-glycero-3-cytidine nucleolipid, polarization modulation infrared reflection absorption spectroscopy (PM-IRRAS).

Abbreviations
density functional theorem (DFT)
differential capacitance (DC)
1,2-dipalmitoyl-*sn*-glycero-3-cytidine diphosphate (16:0 CDP DG)
Fourier self-deconvolution procedure (FSD)
hybrid bilayer lipid membrane (hBLM)
Langmuir Shafer technique (LS)
nucleolipid (NL)
photoelastic modulator (PEM)
photon polarization modulation infrared reflection absorption spectroscopy (PM-IRRAS)
second derivative (SD)
self-assembled monolayer (SAM)
saturated calomel electrode (SCE)
second derivative (SD)
tabletop optical module (TOM)

1. Introduction

Molecular recognition reaction taking place at an electrode surface plays an important role in the development of drug delivery or biosensor systems where the potential is commonly controlled.[1] The voltage controlled adsorption and co-adsorption of nucleobases at gold electrode surfaces have been extensively investigated.[2–7] However, when the base molecules are directly adsorbed onto the electrode, it is difficult to separate base-base interactions from the base-gold interactions. In a recent paper, a monolayer of 1,2-dipalmitoyl-sn-glycero-3-cytidine was deposited on gold (111) surface[8]. In this architecture, the two long acyl chains of the nucleolipid separate the cytosine moiety from the gold electrode surface eliminating the base-gold interactions and the cytidine head group is oriented toward the solution making it accessible for guanine base pairing.[8] Several studies have also demonstrated that molecular recognition can be conveniently investigated by spreading nucleolipid monolayers at the air-water interface.[9–12] Recently, PM-IRRAS spectroscopy was employed to investigate the potential

controlled orientation of DNA duplexes tethered the gold electrode surface. [13] Therefore, we have applied combination of electrochemical and photon polarization modulation spectroscopy (PM-IRRAS) to investigate the interaction of guanine with a monolayer of 1,2-dipalmitoyl-sn-glycero-3-cytidine deposited on gold (111) surface. These studies revealed that the binding of guanine to the nucleolipid monolayer is strongly potential dependent.[14] However, the complex formation was strongly dependent on the charge density at the metal. In addition, guanine has a strong affinity to the gold electrode surface. In contrast, the physical adsorption interactions between the nucleolipid acyl chains and the gold surface are weak. Figure 1 shows that the PM-IRAS spectrum of 1,2-dipalmitoyl-sn-glycero-3-cytidine monolayer with co-adsorb guanine, in the 1800-1600 cm^{-1} region, is significantly different than the transmission spectrum of a 1,2-dipalmitoyl-sn-glycero-3-cytidine vesicle solution incubated with guanine. This spectral region contains information about the C=O vibrational groups, which are involved in cytosine-guanine complex formation. The spectral differences suggest that guanine may actually penetrate deeply into the 1,2-dipalmitoyl-sn-glycero-3-cytidine monolayer when the monolayer is physisorb to the surface of an electrode.

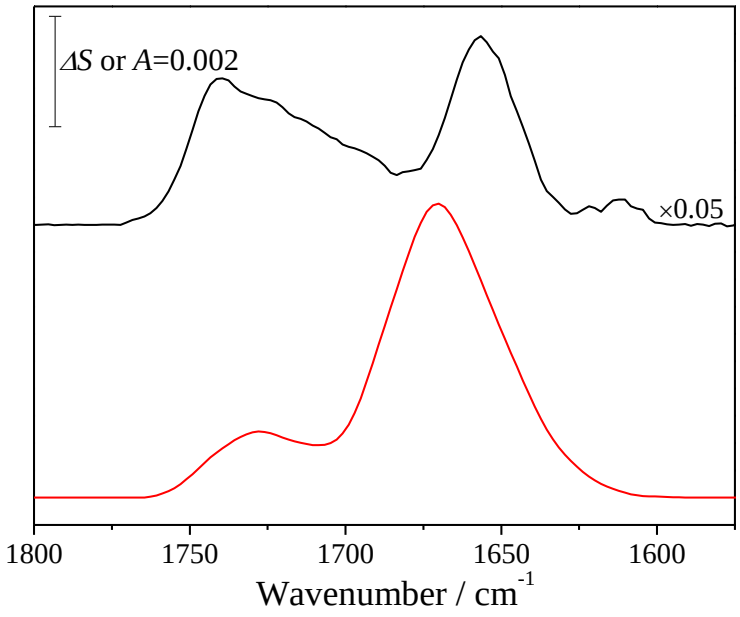

Figure. 1 Average PM-IRRAS spectrum of the nucleolipid (NL) monolayer incubated with 25 μM guanine solution (red) and transmission IR spectrum of NL vesicles in 0.1 M NaF plus 25 μM guanine solution (black).

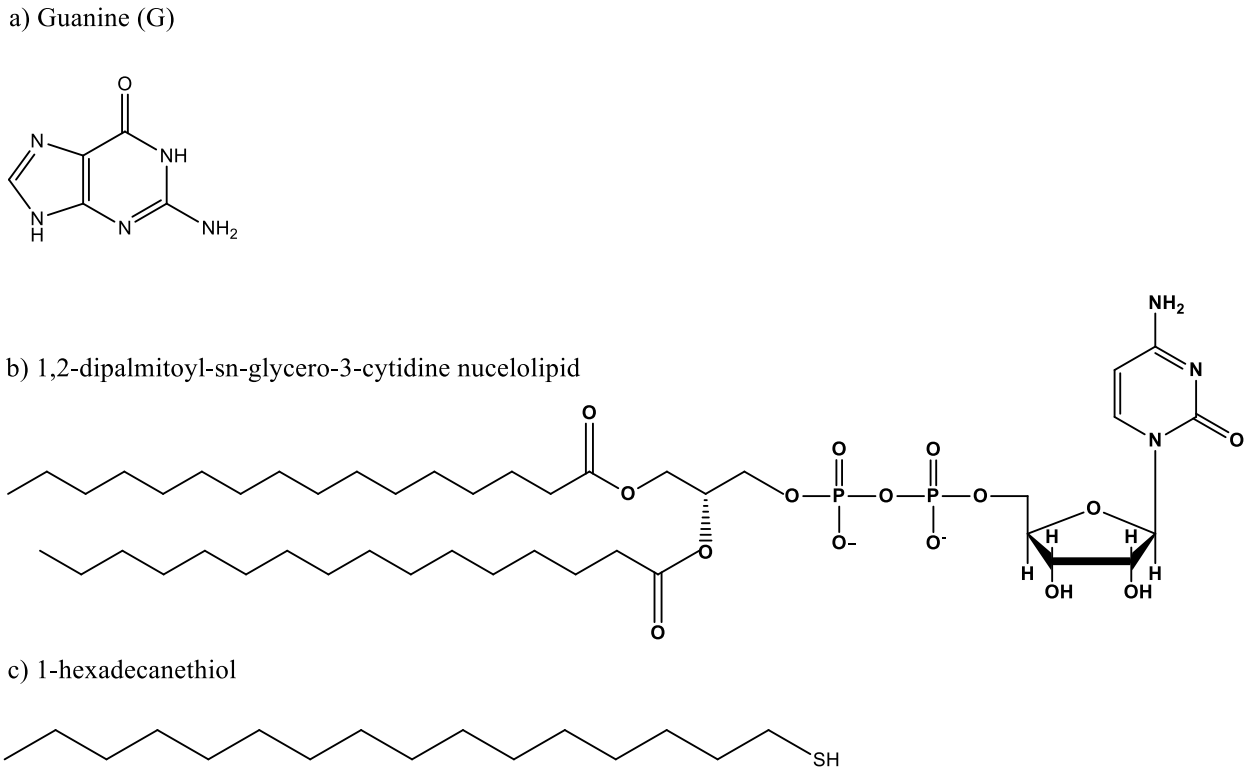

Figure. 2 Molecular structure of a) guanine (G), b) 1,2-dipalmitoyl-sn-glycero-3-cytidine nucleolipid and c) 1-hexadecanethiol.

To prove that the guanine molecules did not displace the nucleolipids within film, we have assembled a hybrid bilayer membrane (hBLM), as shown in Figure 2, where the inner leaflet consisted of a 1-hexadecanethiol self-assembled monolayer (SAM) and the outer leaflet was formed by depositing a monolayer of 1,2-dipalmitoyl-sn-glycero-3-cytidine using the Langmuir Schaefer (LS) technique. The dipole moment of guanine is 6,5D and hence the molecule is quite polar. The long chain of hexadecanethiol created thick nonpolar region in which lipids are in the gel state, preventing penetration of guanine molecules below the polar head region. This hBLM is highly robust and eliminates the direct interaction between gold and guanine due to the strong affinity of the gold-sulfur bond. The objective of this paper was to characterize the interaction between cytidine and guanine using the hBLM system. This architecture allows better packing of the lipids and permits studies of the interaction between the two complementary bases in a broader range of potentials. Electrochemical measurements were used to monitor the stability of the hBLM and PMI-IRRAS spectra to provide information about

the orientation of the acyl chain, the cytidine nucleolipid as well as the interaction between cytidine and guanine. The information gained in this study is relevant for the development of molecular sensors in the future.

2. Material and methods.

2.1. Reagents, solutions, electrodes and materials.

1,2-dipalmitoyl-s*n*-glycero-3-cytidine diphosphate (16:0 CDP DG), was purchased from Avanti Polar Lipid and dissolved in chloroform to give a 1 mg mL^{-1} stock solution. The 1-hexadecanethiol obtained from Merck was dissolved in methanol to obtain a 1 mg mL^{-1} stock solution. Sodium fluoride powder (BioXtra, 99%) obtained from Sigma-Aldrich was cleaned in a UV ozone chamber (UVO cleaner, Jelight) during 15 minutes in order to oxidize any organic impurities prior to electrolyte preparation. For electrochemical measurements, all aqueous electrolytes solutions were prepared using ultrapure water (resistivity > 18.2 M) from a purified Milli-Q UV plus (EMD Millipore) water system. D_2O (Cambridge Isotope Laboratories) was employed for electrolytes solutions for PM-IRRAS.

Home-grown single crystal gold (111) electrodes were used as the working electrode and Ag/AgCl (saturated KCl, Pine Research Instrumentation) were employed as a reference electrode in both PM-IRRAS and electrochemical experiments. Prior to each measurement the single crystal gold (111) electrode was flame-annealed and cooled in air. A platinum (Pt) foil was used as the counter electrode in PM-IRRAS experiments while the flame-annealed gold coiled wire was employed as a counter electrode in the electrochemical measurements. Spectroelectrochemical experiments were performed at room temperature (20 ± 2 °C). All potentials are reported versus the saturated calomel electrode (SCE) by converting the measured potentials into the SCE scale. The potential difference between the SCE and Ag/AgCl electrodes is (-0.045 V). Since the goal of this study was to describe the molecular recognition reaction (not to build a sensor), the experiments were performed with 0.025 mM guanine concentration. It is close to the saturation concentration and hence ensured the fastest mass transport to the electrode.

All glassware was cleaned in a potassium permanganate bath overnight or cleaned in a mixed concentrated hot acid bath (3:1 H_2SO_4/HNO_3 v/v) for 2h. Then the glassware was

meticulously rinsed with copious amount of Milli-Q water. The PTFE components of the spectroelectrochemical cell were cleaned in piranha solution (3:1 H_2SO_4/H_2O_2 v/v) and thoroughly rinsed with Milli-Q water.

2.2. Assembly of 1-hexadecanethiol/1,2-dipalmitoyl-sn-glycero-3-cytidine bilayer at the gold (111) surface.

The 1-hexadecanethiol/1,2-dipalmitoyl-sn-glycero-3-cytidine hybrid bilayer was constructed on the gold (111) electrodes by self-assembly of 1-hexadecanethiol monolayer (inner leaflet) followed by a Langmuir-Schaefer (LS) deposition of the 1,2-dipalmitoyl-sn-glycero-3-cytidine monolayer (outer leaflet). The gold electrode was flamed-annealed and immersed into a 1mg mL^{-1} metanolic 1-hexadecanethiol solution at $27 \pm 3°C$ for 12 h ensuring the formation a uniform 1-hexadecanethiol SAM. The electrode was then washed with methanol to remove any physically adsorbed thiol molecules followed by a Milli-Q water rinse to remove residual methanol. The electrode was allowed to dry in argon for 1 h to allow to ensure that no water remained on the SAM surface before depositing the outer, 1,2-dipalmitoyl-sn-glycero-3-cytidine layer using the LS method as previously described.[14] After assembly of the hBLM the electrode was dried in argon for 1h.

2.3. Electrochemical instrumentation and measurements.

Electrochemical measurements were performed using a computer-controlled HEKA PG 590 potentiostat/galvanostat and a lock-in amplifier (EG & G Instruments 7265 DSP). All data were collected using a plug-in acquisition card NI-PCI-6052E and custom written software.

The electrochemical measurements were carried out in an all-glass three-electrode cell using the hanging meniscus configuration. Before applying a potential to the working electrode, the cell was purged with argon for 30 minutes to prevent the influx of oxygen. The purity of 0.1 M NaF electrolyte was verified by recording differential capacitance curves (DC) of the gold (111) electrode and comparing them to curves previously reported in the literature.[15–17] Measurements of differential capacitance (DC) curves of the hybrid bilayer on the gold(111) electrode were performed using a scan rate of 5 mV s^{-1} superimposed on a 5 mV ac perturbation

at a frequency of 25 Hz. The capacitance was calculated treating the electrochemical interface as a series RC circuit. During the measurement, argon was maintained over the solution.

The immersion method as described in the literature [18–22] was employed to determine the potential of zero double layer charge (E_{pzdlc}). A freshly prepared 1-hexadecanethiol/1,2-dipalmitoyl-sn-glycero-3-cytidine bilayer on gold(111) in absence or presence of guanine was placed into the electrochemical cell. The electrode was connected to the potentiostat at a preselected potential. Then the electrode was brought into contact with the electrolyte and the current flowing (double layer charging current) was measured as a function of time. Finally, the charge at the immersion potential was calculated by integrating the current transients. At each potential, data for two independent measurements were averaged. The upper and lower values were used to determine the error bars.

2.4. Spectra collection and processing.

2.4.1. PM-IRRAS spectra.

PM-IRRAS measurements were performed using a Nicolet Nexus 870 (ThermoFisher) spectrometer equipped with an external tabletop optical mount, an MCT-A detector, a photoelastic modulator (Hinds Instruments PM-90 with a II/ZS50 ZnSe 50 kHz optical head) and a sampling demodulator (GWC Instruments Synchronous Sampling Demodulator). The tabletop optical module (TOM) box was purged with dry (CO_2 free) air, provided by a FTIR purge gas generator (Parker Balston) for ~5 h prior to and throughout the duration of the experiment. The spectra were acquired at a temperature of 20 ± 2 °C using an in-house software, an Omnic macro, and a digital-to-analog converter (Omega) to control the potentiostat (EG&G PAR362). The IR window was a 1 in. CaF_2 equilateral prism (Boxin Photoelectric Co.) washed with methanol and water and cleaned in an UV ozone chamber for 10 min before each experiment.

The electrode was transferred to the spectroelectrochemical cell filled with 0.1 M NaF in D_2O. The electrolyte was de-aerated with argon for 20 min to remove the O_2. The electrode was then pressed against the IR prism creating a thin film configuration. The electrode potential was changed from 0.36 V vs SCE to -0.75 V vs SCE in steps of 0.1 V. The IR spectra at each potential were generated by averaging 4000 scans to provide an adequate signal to noise ratio with an instrument resolution of 4 cm^{-1}. The PM-IRRAS measurements were performed at an

incidence angle of 60^{o} with the photoelastic modulator (PEM) set to a half-wave retardation of 1600 cm^{-1} to obtain a large enhancement of the mean square electric field strength (MSEFS) of p-polarized radiation at the electrode surface. The electrolyte thickness was ~4 μm, which was determined as previously described in the literature.[23]

In the PM-IRRAS experiment, ΔS is measured, which after correction for PEM response functions is proportional to the absorbance, A, of the molecules adsorbed on the electrode surface and defined as:

$$\Delta S = \frac{2(I_s - I_p)}{I_s + I_p} = 2.3\varepsilon\Gamma \quad (1)$$

where I_s and I_p are the intensities of the s- and p-polarized radiation, Γ is the surface concentration of the adsorbed species and ε is the decadic molar absorption coefficient of the adsorbed species. The details of PM-IRRAS measurement and data processing were described previously. [23-25]

2.4.3. Simulation of the PM-IRRAS spectra of the hybrid bilayer.

The PM-IRRAS spectra of 1-hexadecanethiol/1,2-dipalmitoyl-sn-glycero-3-cytidine bilayer on gold(111), were simulated using a model of five homogeneous parallel phases (Au/1-hexadecanethiol/1,2-dipalmitoyl-sn-glycero-3-cytidine/D_2O/CaF_2) and an in house made software to solve the Fresnel equation using the transfer matrix method.[25] The optical constant of Au, D_2O and CaF_2 were taken from the literature.[26–28] The optical constant of the 1-hexadecanethiol and the 1,2-dipalmitoyl-sn-glycero-3-cytidine nucleolipid were obtained from the transmission spectra. The thickness of the 1,2-dipalmitoyl-sn-glycero-3-cytidine nucleolipid was assumed to be 3 nm which is equal to a half of the thickness of DPPC bilayer[29]; the thickness of the 1-hexadecanethiol was taken as 2.5 nm [30].

3. Results and discussion.

3.1. Electrochemical measurements.

Differential capacitance (DC) curves were used to determine the behavior and stability of the hybrid 1-hexadecanethiol/1,2-dipalmitoyl-sn-glycero-3-cytidine bilayers in the absence and

presence of guanine, as a function of the applied potential. Figure 3 compares the DC curves of the pure gold (111) electrode in 0.1 M NaF (1), the gold (111) electrode covered with a SAM of 1-hexadecanethiol (2) and the 1-hexadecanethiol/1,2-dipalmitoyl-sn-glycero-3-cytidine bilayer in presence (3) and absence (4) of guanine as a function of the applied potential. The minimum of capacity for the hybrid bilayers (~ 0.97 μF cm^{-2} in the presence of guanine and ~ 0.84 μF cm^{-2} in the absence of guanine) are slightly smaller than the minimum capacity to the gold (111) electrode covered only by a SAM of 1-hexadecanethiol (~ 1 μF cm^{-2})[30] confirming that well-ordered and densely packed bilayers are formed on the electrode. Moreover, these bilayers are stable in a broader range of potentials (from -1 V to 0.4 V vs SCE) than the 1-hexadecanethiol monolayer films where electro-dewetting of the SAM begins at -0.8 V vs SCE compared to -1.0 v vs SCE for the hBLM systems.

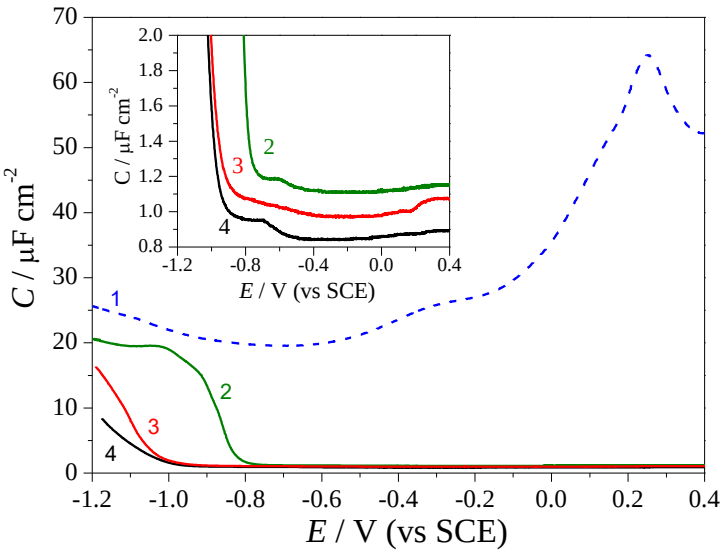

Figure. 3 Differential capacitance curves for bare gold (111) electrode (1-blue dashed line), 1-hexadecanethiol SAM-modified gold electrode (2-solid green line), 1-hexadecanethiol/1,2-dipalmitoyl-sn-glycero-3-cytidine bilayers on gold (111) electrode in presence (3-solid red line) and absence (4-solid dark line) of guanine in 0.1 M NaF electrolyte. Inset expanded sensitivity showing differences in the differential capacitance.

The immersion method, described by Hamm et al. [18–22], has been used to determine the potential of zero double layer charge (E_{pzdlc}) for the gold (111) electrode with 1-hexadecanethiol/1,2-dipalmitoyl-sn-glycero-3-cytidine bilayers in presence and absence of

guanine. The bilayer covered surface of the gold (111) electrode was oriented horizontally to electrolyte surface. The electrode was slowly brought into the contact with the electrolyte at a controlled potential. When the contact was made, a current of charging the double layer flows through the electrode. Figure S1 of the Supporting Information shows typical current transients recorded when the contact between the electrode and the solution was made. The integration of the transient gives the charge density at the immersion potential (Equation 2):

$$\sigma_M = \int_0^\infty i(E,t)dt \tag{2}$$

where i is the capacitive current density and t is the time elapsed from the moment of solid-liquid interface formation. The immersion method measures ionic charge flowing to the interface to compensate the charge on both the metal and film present at the metal surface. In the case of a film consisting of electroneutral molecules, this method measures the potential of zero free charge on the metal. In the case of a film composed of negatively charged molecules (as in the present case), the immersion method can be used to determine the potential of zero double layer charge where the combined charge of the film and metal is equal to zero.

Figure 4a and b plot the charge density (σ_M) determined for several immersion potentials for the electrode covered by the hBLM in the absence and presence of guanine. A linear regression applied to the data, gives slopes equal to 0.7 μFcm^{-2} in the absence and 0.91 μF cm^{-2} in presence of guanine, respectively. These double layer capacitance values are in a good agreement with the values measured by differential capacitance in Figure 3. The charge density curves intersect the zero line at: 0.13 ± 0.03 V vs SCE in the absence and at 0.17 ± 0.03 V vs SCE in the presence of guanine. These numbers correspond to potentials of zero charge of the double layer (E_{pzdlc}). The differences between these numbers are small and almost within limits of experimental error.

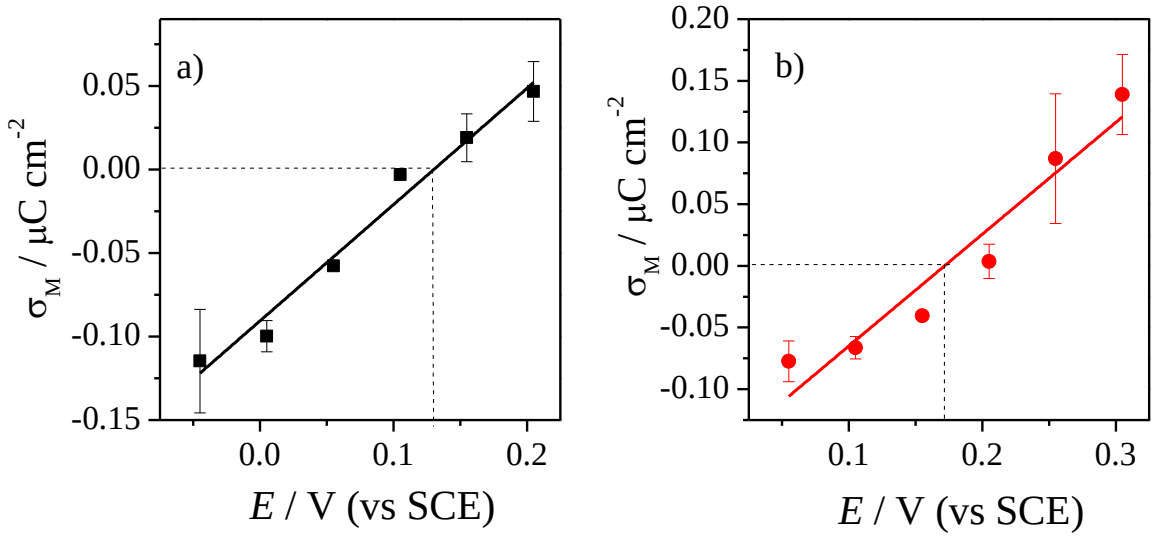

Figure. 4 Charge density determined by integration of the current flowing to the gold electrode covered with the 1-hexadecanethiol/1,2-dipalmitoyl-sn-glycero-3-cytidine bilayer in the a) absence and b) presence of guanine when the electrode was brought in contact with 0.1 M NaF electrolyte solution at the plotted applied voltage.

3.3. PM-IRRAS measurements

PM-IRRAS spectra were used to provide information about the orientation and conformation of 1,2-dipalmitoyl-sn-glycero-3-cytidine leaflet formed on the 1-hexadecanethiol-SAM modified gold (111), either in the presence or absence of guanine. The outer leaflet of 1,2-dipalmitoyl-sn-glycero-3-cytidine nucelolipid was transferred from the air-solution interface to the 1-hexadecanethiol SAM modified gold(111) surface at of 30 mN m^{-1}. At this surface pressure, the film is in the liquid-crystalline state (Figure S2). Since the C-H vibrations of the SAM and the nucleolipid chains overlap, the IR bands corresponding to the chains vibrations give only the average of structural properties of the two leaflets. The spectra for the C-H stretch region are presented in the Supporting Information (Figures S3 & S4 and Tables S1 & S2). In this study, we are primarily concerned with properties of the top leaflet of the nucleolipid, therefore, analysis of this IR region will be discussed in further detail.

3.3.1 Polar head region 1800-1400 cm^{-1}.

The spectral region from 1800 to1400 cm^{-1} contains information concerning the orientation and conformation of the polar head group fragment of the molecule. It also provides information concerning molecular recognition between cytidine and guanine. The bands associated with CH bending, CN stretching and CO stretching are located in this region.

Figure 5 shows the average PM-IRRAS spectrum of the hybrid bilayer with 1-hexadecanethiol/1,2-dipalmitoyl-sn-glycero-3-cytidine diphosphate without (a) and with (b) guanine. The intensities of the average PM-IRRAS spectrum of the bilayer are significantly different when guanine is present. The bands at ~1730 cm^{-1} correspond to the carbonyl group vibration of the glycerol moiety of 1,2-dipalmitoyl-sn-glycero-3-cytidine. The intensity of this band provides information about the angle θ between the direction of the transition dipole of a corresponding vibration and surface normal. It can be calculated using the equation [23]:

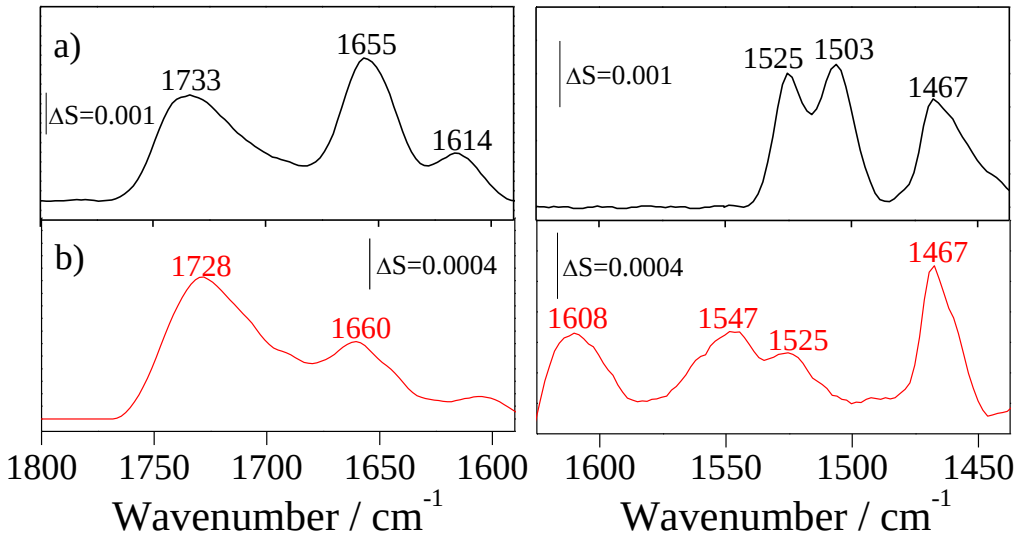

Figure. 5 1800-1400 cm^{-1} region in D_2O/NaF for average PM-IRRAS spectra of a) 1-hexadecanethiol/1,2-dipalmitoyl-sn-glycero-3-cytidine diphosphate bilayer without guanine and b) 1-hexadecanethiol/1,2-dipalmitoyl-sn-glycero-3-cytidine diphosphate bilayer with guanine.

$$\frac{\int A_{exp} d\bar{\upsilon}}{\int A_{cal} d\bar{\upsilon}} = \frac{cos^2\theta}{cos^2 55} \quad (3)$$

where $\int A_{exp} d\bar{\upsilon}$ and $\int A_{cal} d\bar{\upsilon}$ are the integrated intensities for the PM-IRRAS experimental band and for the theoretical spectrum of randomly oriented molecules calculated from optical

constants, respectively. In the case of C=O band, the direction of the transition dipole coincides with the bond direction. Figure 6 plots the average angles between the directions of the C=O bonds and the surface normal. The angles are noticeably higher when guanine is introduced to the system. The angle between direction of the C=O group and fully extended all *trans* acyl chain is ~90^{o}. [31] Therefore, the average angle of the C=O bonds, reported in Figure 6, suggest that acyl chains of 1,2-dipalmitoyl-sn-glycero-3-cytidine diphosphate leaflet are tilted by about 20^{o} and 15^{o} with respect to the surface normal in the absence and presence of guanine, respectively.

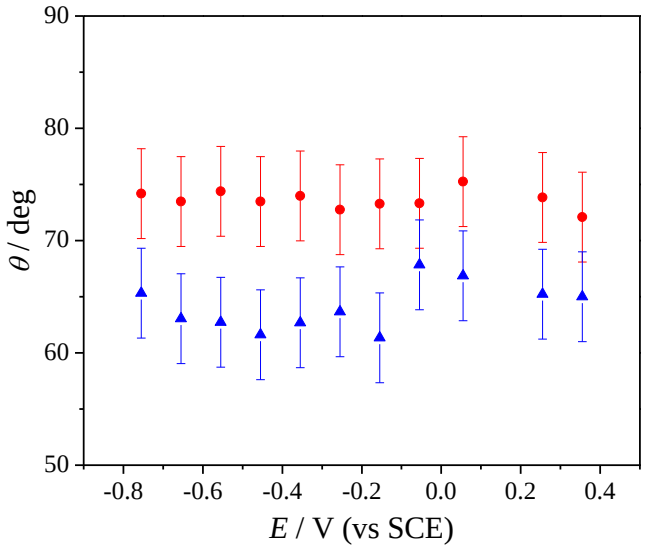

Figure. 6 Tilt angle of the C=O bond for the 1-hexadecanethiol/1,2-dipalmitoyl-sn-glycero-3-cytidine hybrid bilayer with (red circles) and without (blue triangles) guanine.

The wide bands in this region are associated with the C=O vibrations of cytidine and guanine and can provide information about the complex formation. The intensities of the bands in this region are weaker in the presence of guanine. The spectral region between 1600 and 1500 cm^{-1} contains more bands in the presence of guanine indicating that guanine molecules are attached to the hybrid bilayer. In the presence of guanine, the intensities of bands due to guanine and cytosine are comparable indicating that the ratio of guanine and cytosine in the bilayer is close to one. This relationship was also observed in our previous work involving 1,2-dipalmitoyl-sn-glycero-3-cytidine diphosphate monolayers adsorbed to the gold (111) electrode surface in presence of guanine. [14]

The Fourier self-deconvolution (FSD) procedure (Figures 7b and 9b) was employed to reveal the sub-band structure of the average PM-IRRAS spectrum of 1-hexadecanethiol/1,2-dipalmitoyl-sn-glycero-3-cytidine diphosphate bilayer on gold (111) in the absence and presence of guanine. The FSD narrows the IR bands within the broad spectral envelope resolving complex spectral features making it possible to identify the number and position of the bands used in the spectral deconvolution shown in Figures S5 and S6 of the Supporting Information. [32] The band assignment for each vibrational frequency has been summarized in Table 1.

Table. 1 Bands observed in PM-IRRAS average spectra of 1,2-dipalmitoyl-sn-glycero-3-cytidine monolayer and 1-hexadecanethiol/1,2-dipalmitoyl-sn-glycero-3-cytidine bilayer in presence and absence of guanine in 1800-1400 cm^{-1} region in D_2O/0.1 M NaF. [8] ,[14]

No Guanine		**With Guanine**		**Band Assignment**[8], [14]
Monolayer[8]	**Hybrid**	**Monolayer**[14]	**Hybrid**	
1736	1739	1741	1741	$\nu C=O_{(hydrogen\ non\text{-}bonded)\ glycerol}$
1722	1723	1728	1729	$\nu C=O_{(hydrogen\ bonded)\ glycerol}$
		1689	1690	C≡G complex
		1670	1674	νC=O guanine
			1660	Guanine skeletal
1646	1655	1648	1643	$\nu C=O_{cytosine}$
			1625	C≡G complex
1612	1614			$\nu C5=C6_{cytosine}$
		1598	1608	cytosine
		1574	1565	Guanine skeletal
		1550	1547	Guanine skeletal
1523	1525	1523	1525	νC4=C5cytosine
1505	1503	1502		νC4=N7cytosine
1467	1467	1467	1467	δCH_2

All band positions are reported in cm^{-1}

3.3.2.1 Potential dependent changes in the IR spectra of the polar head group in the absence of guanine

The PM-IRRAS spectra of the hybrid bilayer were recorded in the range of potentials between -0.75 V and 0.36 V vs SCE. Figure 7a shows the PM-IRRAS spectra in the 1800-1400 cm^{-1} region determined at selected potentials.

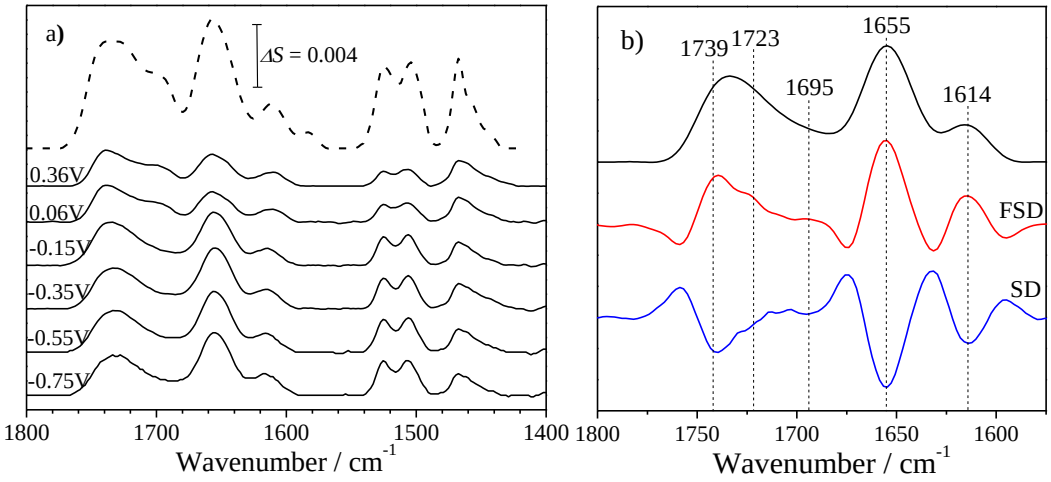

Figure. 7 a) PM-IRRAS spectra of the 1-hexadecanethiol/1,2-dipalmitoyl-sn-glycero-3-cytidine diphosphate bilayer at the gold (111) surface in 1800 - 1400 cm^{-1} region at selected potentials. The top dashed line is the transmission IR spectrum of 1,2-dipalmitoyl-sn-glycero-3-cytidine vesicles in 0.1 M NaF. b) Fourier self-deconvolution (red, FSD) and second derivative (SD, blue) results of the average PM-IRRAS spectrum of the 1-hexadecanethiol/1,2-dipalmitoyl-sn-glycero-3-cytidine diphosphate bilayer in the 1800-1575 cm^{-1} region.

Equation 3 can be used to calculate the angle θ between the direction of the transition dipole moment and surface normal from the integrated intensities of the IR bands. Recently two papers, [8] and [14], demonstrated that the tilt angle of cytosine molecular plane relative to the surface normal (α) and the angle between the transition dipole and the projection of the surface normal on the molecular plane (φ) can be determined, if the transition dipole angles θ for the 1525 and 1503 cm^{-1} bands are known. In addition, the DFT calculations have to be performed to determine the difference between angles φ of the two in-plane vibrations ($|\varphi_1-\varphi_2|$). The angle φ provides information about rotation of the molecular plane of the molecule. The angles, θ, α and φ are related by the expression [2,8,14]:

$$\cos(\theta) = \cos(\alpha) \times \cos(\varphi) \qquad (4)$$

Figure 8a plots the angles of transition dipoles of the 1525 and 1503 cm^{-1} bands corresponding to in-plane vibrations of the cytosine moiety in absence of guanine. The angles change from ~67º at potentials more positive than the E_{pzdlc} to ~55º at more negative potentials. The interpretation of the angle equal to ~55º is not unique as it may correspond to random orientation. However, the changes in the transition dipole angle of θ of 1525 and 1503 cm^{-1} bands shown in Figure 8a may also correspond to changes of the tilt of molecular plane shown in Figure 8b, which also changes from 60º to 45º when the potential is scanned from positive to negative potentials.

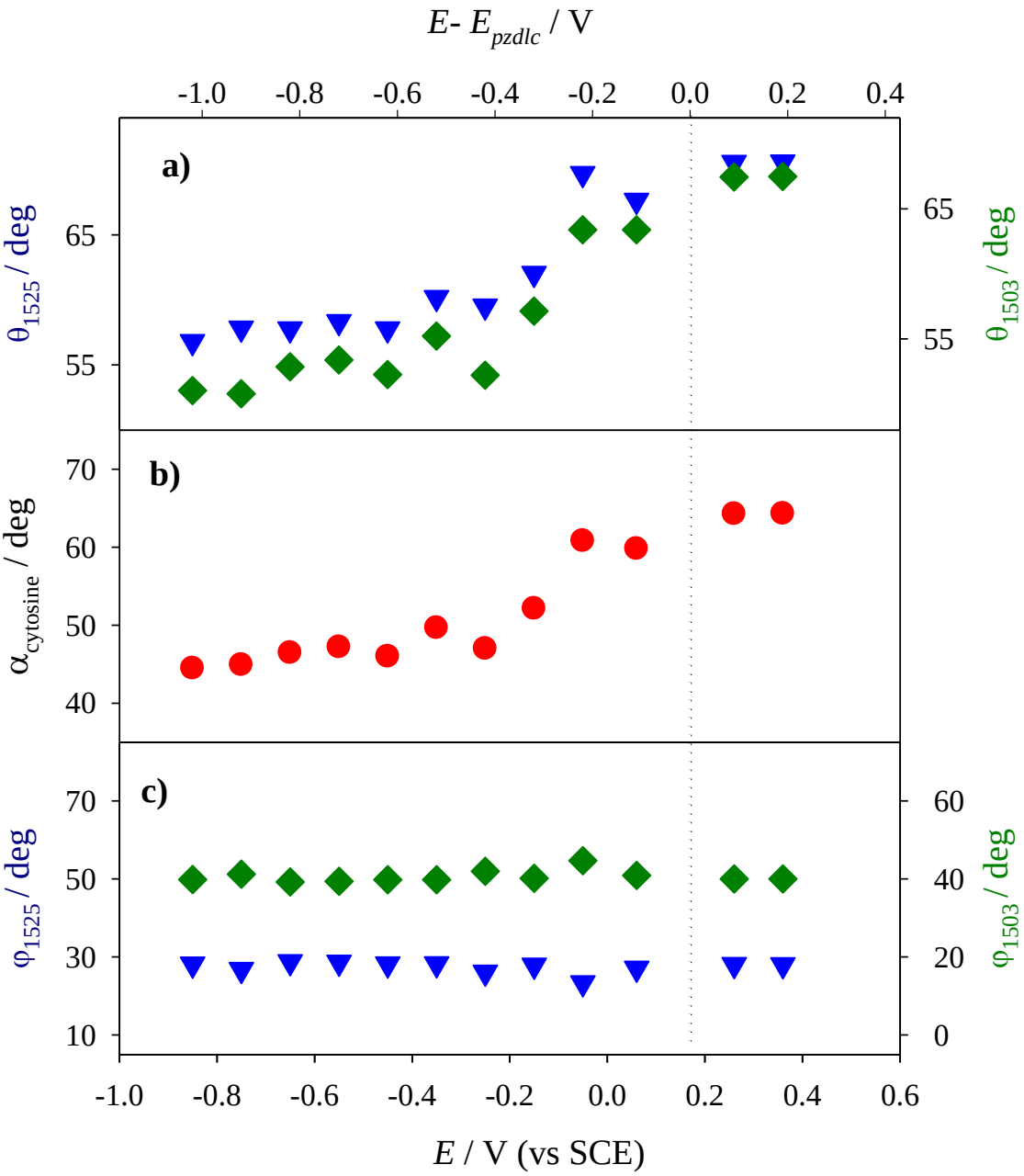

Figure. 8 a) Angles between direction of transition dipole moments and the surface normal corresponding; b) tilt angle of the molecular plane relative to the surface normal, c) angles between the transition dipole and the projection of the surface normal on the molecular plane (φ), plotted as a function of applied potential, for 1525 cm^{-1} (blue triangles) and 1503 cm^{-1} (green diamonds) bands of the cytosine moiety in the hybrid bilayer without guanine

Since similar changes of θ are observed for the two IR bands, it suggests that the tilt angle of the molecular plane takes place without undergoing any rotation. Interestingly, the behavior of the cytosine moiety in the hybrid bilayer is different from the physisorbed monolayer described in our previous work [8]. In the monolayer, the plane of the cytosine moiety was more parallel with respect to the electrode surface and rotated from ~70^{o} at positive potentials to ~50^{o} at negative potentials. Tentatively, this difference could be explained by a stronger influence of the static electric field on the cytosine moiety in the monolayer than in the hybrid bilayer.

3.3.2.2 Potential dependent changes in the IR spectra of the polar head group in the presence of guanine

Figure 9a shows PM-IRRAS spectra in 1800-1575 cm^{-1} region of the 1-hexadecanethiol/1,2-dipalmitoyl-sn-glycero-3-cytidine diphosphate bilayer in presence of guanine. The FSD and second derivate analysis of the broad PM-IRRAS bands located in the 1725-1575 cm^{-1} region are presented in Figure 9b along with a transmission spectrum (dotted line) of the polyC:polyG complex. The FSD spectra show bands at 1690 and 1643 cm^{-1}, which also appear at 1688 and 1647 cm^{-1} in polyC:polyG transmission spectrum [33] suggesting that the Watson-Crick complex between guanine and cytosine has been formed.[33,34] However, the strong IR band present at 1660 cm^{-1} indicates that non-complexed guanine also exists within the bilayer.

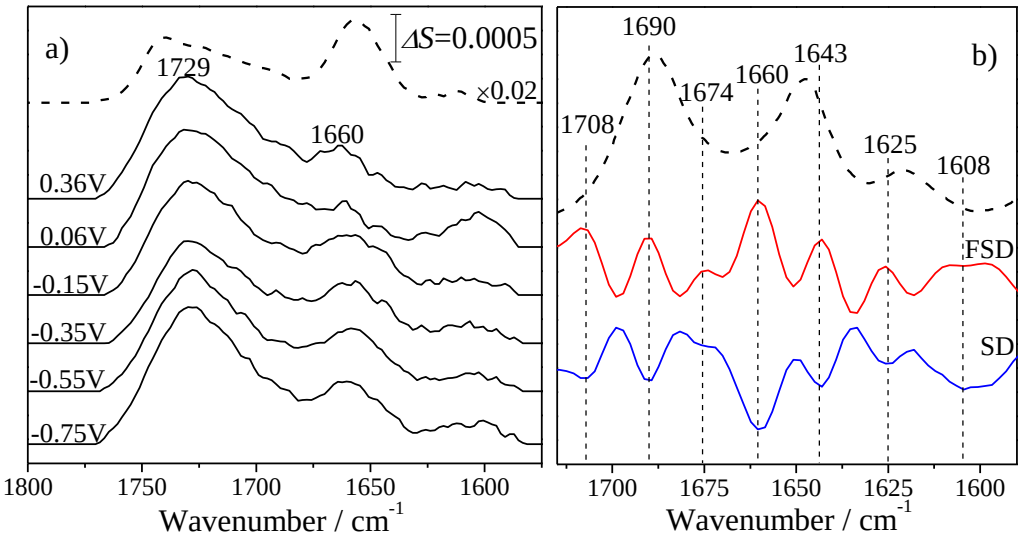

Figure. 9 a) PM-IRRAS spectra of the 1-hexadecanethiol/1,2-dipalmitoyl-sn-glycero-3-cytidine diphosphate bilayer in presence of guanine in 1800 - 1575 cm^{-1} region at the gold (111) at selected potentials. The top dashed line is the transmission IR spectrum of 1,2-dipalmitoyl-sn-glycero-3-cytidine vesicles in 0.1 M NaF with guanine. b) Fourier self-deconvolution (red, FSD) and secondary derivative (SD, blue) results of the average PM-IRRAS spectrum of the 1-hexadecanethiol/1,2-dipalmitoyl-sn-glycero-3-cytidine diphosphate bilayer. Dashed curve is the transmission spectrum of PolyC:PolyG complex in D_2O taken from the literature.

With the help of the FSD, the PM-IRRAS spectra were deconvoluted into their individual vibrations shown in Figure S6 of the Supporting Information. The integrated intensities of the 1690, 1660 and 1643 cm^{-1} bands are plotted in Figure 10 as a function of the electrode potential. The integrated intensities of the 1690 cm^{-1} band, corresponding to the complex-forming guanine, are potential independent indicating that the complex exists at all measured potentials. The IR band located at 1660 cm^{-1}, which correspond to non-complexed guanine (or non-coupling interactions between guanine and cytosine), and the band located at 1643 cm^{-1} corresponding to the free cytosine moiety increase when the potentials is moved from positive to negative values. Figure S7 of the Supporting Information plots the ratio of the integrated intensity of the 1690 and 1660 cm^{-1} bands. This ratio can be used to roughly measure the amount of C:G complex at the electrode surface. The ratio changes from 0.8 at positive potentials to 0.6 at the negative end of potentials. These values are much higher than those of the physisorbed monolayer [8] where the 1690/1660 ratio varied from 0.35 to nearly zero. Apparently, C:G complexation occurs more readily in the hybrid bilayer and is less affected by the change in electrode potential.

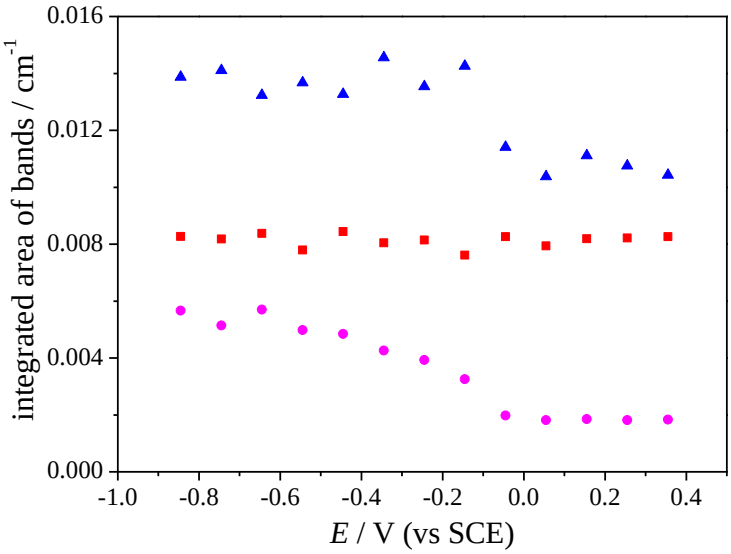

Figure. 10 Integrated intensities of the bands at 1690 (red squares), 1660 (blue triangles) and 1643 cm^{-1} (pink circles).

More information about the orientation of cytosine and guanine moieties could be obtained from the analysis of the 1600-1500 cm^{-1} region shown in Figure 11. All bands are well resolved and correspond to the purine and pyridine rings of guanine and cytosine, respectively. Assignment of these bands is listed in Table 1 and discussed in our previous paper [14]. The bands are very weak and hence the noise level prevents quantitative analysis of their intensity. However, a remarkable feature is the absence of the band at ~1502 cm^{-1} corresponding to in-plane vibrations of cytosine moiety. This band was quite strong in the spectrum of the bilayer without guanine (Figure 7). It was also present in the spectrum of the monolayer with guanine described in ref [14]. DFT calculations showed that directions of the transition dipoles of the ~1503 and 1643 cm^{-1} bands are close.[14] The absence of the 1502 cm^{-1} band is therefore consistent with the weak intensity of the 1643 cm^{-1} band shown in Figure 10. Despite a high level of noise Figure 11 shows that the intensity of bands in the 1625-1450 cm^{-1} region depends weakly on potential. Therefore, the integrated intensity of the ~1525 cm^{-1} band in the average spectrum was used to evaluate the average orientation of the cytosine moiety. The absence of the ~1502 cm^{-1} was used as the indication that the transition dipole of this band is nearly orthogonal to the electrode surface. For the 1525 cm^{-1} band in the hBLM in the presence of guanine, the average angle between direction of the transition dipole and surface normal (θ) is 75 ± 3°, the tilt angle of the cytosine molecular plane (α) is 74 ± 3°and the rotation angle (φ) for this band is

22 ± 3° (90 degrees for 1503 cm^{-1}). These numbers differ significantly from the tilt of the molecular plane and the rotation angles reported above for the hBLM without guanine. However, the tilt of the molecular axis α determined for hBLM is comparable to the average tilt observed for the monolayer with guanine, which varied ~80° to ~75° [14]. In the presence of guanine, the plane of cytosine moiety assumes an orientation nearly parallel to the bilayer (electrode) surface both in the monolayer and hBLM. Although the tilt is similar, different rotations of the molecular plane are observed for the two films. The cartoons in Schematic 1a graphically illustrate the orientations of the cytosine moiety without guanine and the C:G complex at the potentials at the positive and negative ends. The cartoon in Figure 12 b illustrates the predicted orientation of the complex.

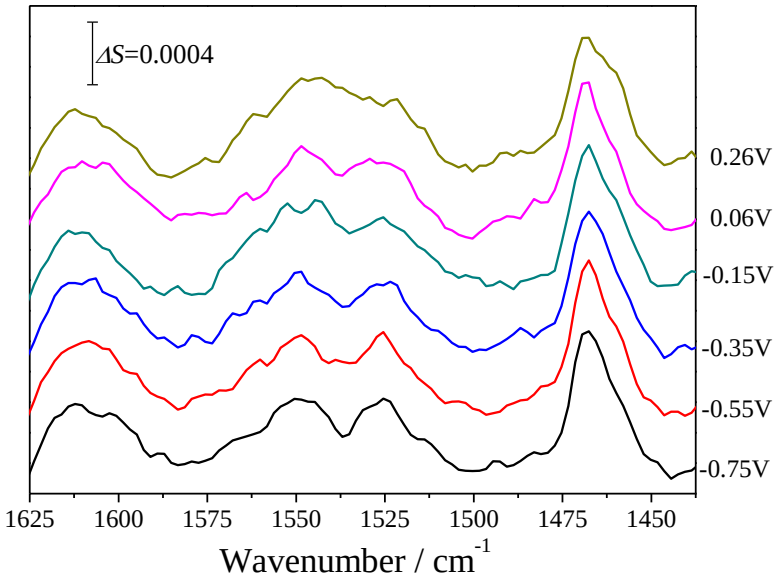

Figure. 11 PM-IRRAS spectra of the 1-hexadecanethiol/1,2-dipalmitoyl-sn-glycero-3-cytidine diphosphate bilayer in presence of guanine in 1650-1425 cm^{-1} region at the gold (111) at selected potentials in presence of guanine in 0.1M NaF/D_2O electrolyte.

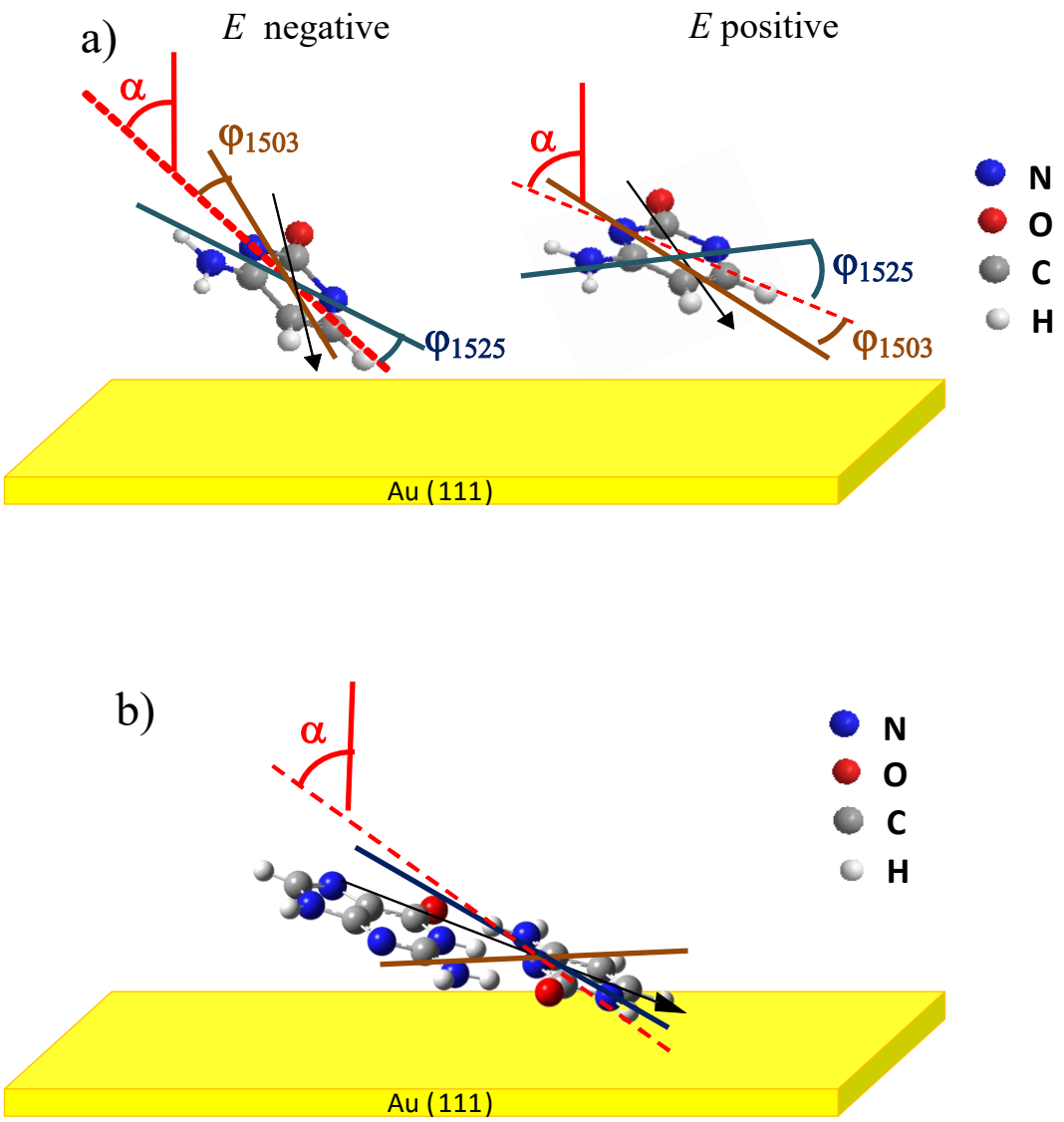

Schematic 1 (a) The electric field driven changes in the tilt and rotation of the plane of cytosine moiety in the hybrid bilayer in the absence of guanine; b) schematic diagram of the orientation of the Watson-Crick complex formed between guanine and cytosine moiety at the hybrid bilayer. The black arrow indicates direction of the permanent dipole moment drawn from negative to positive end, green and blue lines plot directions of transition dipole moments of the 1503 and 1525 cm^{-1} bands. The dashed red line marks projection of the surface normal on the plane of cytosine moiety.

4. Conclusions.

We have compared the guanine-cytosine molecular recognition reaction of a hybrid bilayer, where the inner leaflet consisted of a SAM of the 1-hexadecane thiol and the outer leaflet of a cytosine-containing nucleolipid, with a physisorbed monolayer of the same

nucleolipid molecule deposited directly onto the gold (111) electrode surface as described in [14]. In both films, guanine was present in both the complexed and non-complexed forms, however, the molecular complex between guanine and the cytosine was formed more efficiently at the hybrid bilayer surface since a higher percentage of C:G complex was observed. In addition, the complexation between guanine and cytosine showed a smaller potential dependence in the hybrid bilayer implying that the Watson-Crick complex was more stable on this electrode. In the presence of guanine, the cytosine moiety assumed a nearly parallel orientation with respect to the film surface in both systems, however, the plane of the molecule rotated differently at the monolayer and the bilayer surfaces. The differences between the molecular recognition reactions taking place at the monolayer and the bilayer surfaces can be explained by different influence of the static electric field. The differential capacity of the electrode covered by hBLM is very small (~1 μF cm^{-2}) and an order of magnitude smaller than for the electrode covered by the monolayer. Consequently, the gold electrode has much smaller charge density when it supports hBLM and hence much smaller static electric field is acting on the nucleolipid in the distal leaflet of the bilayer. The hybrid bilayer is a better system for the design of a biochemical sensor. This study gives the following information for the future sensor development: (i) the molecular recognition and hence specificity is improved in the hybrid bilayer architecture, (ii) the complex formation depends weakly on potential and (iii) since changes of the differential capacitance are small the sensor should employ other techniques such as quartz crystal microbalance.

5. Acknowledgements

The FP and MR acknowledge research grants from Spanish Ministry of Economy and Competitiveness (CTQ2014-57515-C2-1-R) and Andalusian government (PAI-FQM202). JL acknowledges support of the Discovery grant from Natural Sciences and Engineering Council of Canada RG-03958. JAM acknowledges a FPU grant and a Visiting Academic grant from the Spanish Ministry of Science and Technology.

6. Supporting Information

Figure S1, Examples of capacitive current transients used to determine E_{pzdlc}. Figure S2, compression isotherms for the 1,2-dipalmitoyl-sn-glycero-3-cytidine in the absence and presence

of nucleolipid in solution. Figure S3 and Figure S4, PM IRRAS spectra in the CH stretching region of the bilayer in the absence and presence of guanine, respectively. Figure S5 and Figure S6, deconvolution of the PM IRRAS spectra of the head group region of the 1,2-dipalmitoyl-sn-glycero-3-cytidine leaflet in the absence and presence of guanine respectively. Figure S7, ratio of the integrated intensity of 1690 and 1660 cm^{-1} bands (complexed/noncomplexed guanine) are presented in the Supporting Information.

References:

[1] D. Bizzotto, I.J. Burgess, T. Doneux, T. Sagara, H. Yu, D. Bizzotto, I.J. Burgess, T. Doneux, T. Sagara, H. Yu, Beyond Simple Cartoons : Challenges in Characterizing Electrochemical Biosensor Interfaces Beyond Simple Cartoons : Challenges in Characterizing Electro- chemical Biosensor Interfaces, ACS Sensors. 3 (2018) 5–12. doi:10.1021/acssensors.7b00840.

[2] F. Prieto, Z. Su, J.J. Leitch, M. Rueda, J. Lipkowski, Quantitative Subtractively Normalized Interfacial Fourier Transform Infrared Reflection Spectroscopy Study of the Adsorption of Adenine on Au(111) Electrodes, Langmuir. 32 (2016) 3827–3835. doi:10.1021/acs.langmuir.6b00635.

[3] F. Prieto, J. Alvarez-Malmagro, M. Rueda, Electrochemical Impedance Spectroscopy study of the adsorption of adenine on Au(111) electrodes as a function of the pH, J. Electroanal. Chem. 793 (2016) 209-217. doi:10.1016/j.jelechem.2017.03.021.

[4] J. Alvarez-Malmagro, M. Rueda, F. Prieto, In situ surface-enhanced infrared spectroscopy study of adenine-thymine co-adsorption on gold electrodes as a function of the pH, J. Electroanal. Chem. 819 (2018) 417–427. doi:10.1016/j.jelechem.2017.11.054.

[5] J. Alvarez-Malmagro, F. Prieto, M. Rueda, A. Rodes, In situ Fourier transform infrared reflection absortion spectroscopy study of adenine adsorption on gold electrodes in basic media, Electrochim. Acta. 140 (2014) 476–481. doi:10.1016/j.electacta.2014.03.074.

[6] M. Rueda, F. Prieto, J. Álvarez-Malmagro, A. Rodes, Evidences of adenine – thymine Interactions at gold electrodes interfaces as provided by in-situ infrared spectroscopy, Electrochem. Commun. 35 (2013) 53–56. doi:10.1016/j.elecom.2013.07.026.

[7] F. Prieto, J. Alvarez-Malmagro, M. Rueda, J.M. Orts, Tautomerism of adsorbed Thymine on gold electrodes: an in situ surface-enhanced infrared spectroscopy study, Electrochim. Acta. 201 (2016) 300–310. doi:10.1016/j.electacta.2015.11.109.

[8] J. Alvarez-Malmagro, Z. Su, J. J. Leitch, F. Prieto, M. Rueda, J. Lipkowski,

Spectroelectrochemical Characterization of 1,2-Dipalmitoyl-sn-glycero-3-cytidine Diphosphate Nucleolipid Monolayer Supported on Gold (111) Electrode, Langmuir. 35 (2019) 901–910. doi:10.1021/acs.langmuir.8b03674.

[9] Y. Wang, X. Du, W. Miao, Y. Liang, Molecular Recognition of Cytosine- and Guanine-Functionalized Nucleolipids in the Mixed Monolayers at the Air - Water Interface and Langmuir - Blodgett Films, J. Phys. Chem. B. 110(10) (2006) 4914–4923. doi:10.1021/jp055046z.

[10] W. Miao, X. Luo, Y. Liang, Molecular recognition of 7-(2-octadecyloxycarbonylethyl)-guanine to cytidine at the air/water interface and LB film studied by Fourier transform infrared spectroscopy, Spectrochim. Acta Part A Mol. Biomol. Spectrosc. 59 (2003) 1045–1050. doi.org:10.1016/S1386-1425(02)00292-5.

[11] W. Miao, X. Luo, S. Wu, Y. Liang, Fourier transform infrared spectroscopy study on order-disorder transition in Langmuir-Blodgett films of 7-(2-octadecyloxycarbonylethyl)guanine before and after recognition to cytidine, Spectrochim. Acta - Part A Mol. Biomol. Spectrosc. 60 (2004) 413–416. doi:10.1016/S1386-1425(03)00240-3.

[12] L. Čoga, L. Spindler, S. Masiero, I. Drevenšek-Olenik, Molecular recognition of a lipophilic guanosine derivative in Langmuir films at the air-water interface, Biochim. Biophys. Acta - Gen. Subj. 1861 (2017) 1463–1470. doi:10.1016/j.bbagen.2016.11.038.

[13] L. Kékedy-Nagy, E.E. Ferapontova, I. Brand, Submolecular Structure and Orientation of Oligonucleotide Duplexes Tethered to Gold Electrodes Probed by Infrared Reflection Absorption Spectroscopy: Effect of the Electrode Potentials, J. Phys. Chem. B. 121 (2017) 1552–1565. doi:10.1021/acs.jpcb.6b12363.

[14] J. Alvarez-Malmagro, Z. Su, J. J. Leitch, F. Prieto, M. Rueda, and J. Lipkowski, Spectroelectrochemical studies of interaction of guanine with 1,2 -Dipalmitoyl-sn-glycero-3- cytidine Diphosphate Nucleolipid Monolayer Supported on Gold (111) Electrode, Langmuir, 35(2019)9297-9307, doi:10.1021/acs.langmuir.9b01238.

[15] N. Garcia-Araez, C.L. Brosseau, P. Rodriguez, J. Lipkowski, Layer-by-Layer PMIRRAS Characterization of DMPC Bilayers Deposited on a Au (111) Electrode Surface, Langmuir. 22(25) (2006) 10365–10371. doi:10.1021/la061217v.

[16] F. Abbasi, J. Alvarez-Mmalmagro, Z. Su, J.J. Leitch, J. Lipkowski, Pore Forming Properties of Alamethicin in Negatively Charged Floating Bilayer Lipid Membranes Supported on Gold Electrodes, Langmuir. 34 (2018) 13754–13765. doi:10.1021/acs.langmuir.8b02554.

[17] D.E.I. L. Stolberg, S. Morin, J. Lipkowski, Adsorption of pyridine at the Au (111) -

solution interface, J. ELectroanal Chem. 307 (1991) 241–262. doi:10.1016/0022-0728(91)85552-Z

[18] P. Ramírez, A. Granero, R. Andreu, A. Cuesta, W.H. Mulder, J. José, Electrochemistry Communications Potential of zero charge as a sensitive probe for the titration of ionizable self-assembled monolayers, Electrochem. Commun. 10 (2008) 1548–1550. doi:10.1016/j.elecom.2008.08.004.

[19] Z. Su, J. Leitch, J. Lipkowski, Measurements of the Potentials of Zero Free Charge and Zero Total Charge for 1-thio- β - D -glucose and DPTL Modified Au (111) Surface in Different, Phys. Chem. Phys. 226 (2012) 995–1009. doi:10.1524/zpch.2012.0280.

[20] R. Andreu, Ä. Cuesta, C.J. Calzado, J. Jose, Determination of the Potential of Zero Charge of Au (111) Modified with Thiol Monolayers, Anal. Chem. 79 (2007) 6473–6479. doi:10.1021/ac071341z.

[21] G. J. Su, M. Homberger, U. Simon, T. Wandlowski, Structure and Electrochemical Characterization of 4-Methyl-4 ′ - (n -mercaptoalkyl) biphenyls on Au (111) - (1×1), J. Phys. Chem. C. 111(46) (2007) 17409–17419. doi:10.1021/jp0744634.

[22] U.W. Hamm, D. Kramer, R.S. Zhai, D.M. Kolb, The pzc of Au (111) and Pt (111) in a perchloric acid solution : an ex situ approach to the immersion technique, J. Electroanal. Chem. 414 (1996) 85–89. doi:10.1016/0022-0728(96)01006-6.

[23] A. Kycia, Z. Su, C. Brosseau, J.Lipkowski. In Situ PM–IRRAS Studies of Biomimetic Membranes Supported at Gold Electrode Surfaces. in "Vibrational Spectroscopy at Electrified Interfaces, ", C. Korzeniewski, B. Braunschweig and A.Wieckowski, (Ed), Wiley-VCH, New York, 2013, pp345-417

[24] V. Zamlynny, PhD thesis, University of Guelph (Canada), 2002.

[25] V. Zamlynny, J. Lipkowski, Quantiative SNIFTIRS and PM IRRAS of organic molecules at electrode surface, in "Advances in Electrochemistry and Electrochemical Engineering", R.Alkire, D.M.Kolb, J.Lipkowski and P.N.Ross (Eds) Vol 9, 2006, pp315-376.

[26] D.L. R.J. Lipert, M. D. Porter, Specular Reflection Spectroscopy, in "Modern Techniques in Applied Molecular Spectroscopy", F.M. Mirabella Ed, Techniques in Analytical Chemistry Series, John Wiley & Sons, Inc., New York 1998.

[27] J.E. Bertie, M.K. Ahmed, H.H. Eysel, Infrared intensities of liquids. 5. Optical and dielectric constants, integrated intensities, and dipole moment derivatives of H_2O and D_2O at 22 degree, J. Phys. Chem., **1989**,93,2210-2218. doi:10.1021/j100343a008

[28] E. Palik, Handbook of Optical Constants of Solids II, Academic Press, San Diego, 1998.

[29] N. Kučerka, Y. Liu, N. Chu, H.I. Petrache, S. Tristram-Nagle, N. Kuc, Nagle, Structure of fully hydrated fluid phase DMPC and DLPC lipid bilayers using X-ray scattering from oriented multilamellar arrays and from unilamellar vesicles. Biophysical Journal, 2005, *88*(4), 2626-2637. doi:10.1529/biophysj.104.056606.

[30] M. D. Porter, T. B. Bright, D.L. Allara, C .E. Chidsey, Spontaneously Organized Molecular Assemblies. 4. Structural Characterization of n-Alkyl Thiol Monolayers, by optical ellipsometry, infrared spectroscopy, and electrochemistry. J.Am.Chem.Soc, 109 (1987) 3559–3568. doi:10.1021/ja00246a011.

[31] X. Bin, I. Zawisza, J.D. Goddard, J. Lipkowski, Electrochemical and PM-IRRAS Studies of the Effect of the Static Electric Field on the Structure of the DMPC Bilayer Supported at a Au (111) Electrode Surface, Langmuir. 21 (2005) 330–347. doi:10.1021/la048710w.

[32] H. Surewicz, W. Mantsch, New Insight into Protein Secondary Structure from Resolution-Enhanced Infrared Spectra, Biochim. Biophys. Acta. 952 (1988) 115–130. doi:10.1016/0167-4838(88)90107-0.

[33] F. B. Howard, J. Frazier, H. T. Miles. Interbase vibrational coupling in G: C polynucleotide helices. Proc. Natl. Acad. Sci., 64(2)(1969) 451-458. doi:10.1073/pnas.64.2.45.

[34] A. T. Krummel, P. Mukherjee, M. T. Zanni, Inter and intrastrand vibrational coupling in DNA studied with heterodyned 2D-IR spectroscopy. J. Phys. Chem. B 107(35) (2003) 9165-9169. doi.org/10.1021/jp035473h.